

CHARACTERIZATION OF THE NEW MALOSSI HYDROTHERMAL SYNTHETIC EMERALD

Ilaria Adamo, Alessandro Pavese, Loredana Prosperi, Valeria Diella, Marco Merlini, Mauro Gemmi, and David Ajò

A new production of hydrothermal synthetic emeralds, grown in the Czech Republic with Italian technology, has been marketed since December 2004 with the trade name Malossi synthetic emerald. Several samples were investigated by standard gemological methods, combined with chemical analyses and UV-Vis-NIR and IR spectroscopy. A comparison of this material with natural and other synthetic emeralds (the latter grown by the flux and hydrothermal techniques) reveals that Malossi hydrothermal synthetic emerald can be identified on the basis of microscopic features and chemical composition, along with the mid-infrared spectrum.

Because of emerald's commercial value, a remarkable number of synthetic emeralds, grown by flux and hydrothermal processes, have entered the market over the past five decades. The hydrothermal synthetic emeralds are particularly notable in terms of the quantity produced and their availability (see, e.g., Kane and Liddicoat, 1985; Koivula et al., 1996; Schmetzer et al., 1997; Koivula et al., 2000; Chen et al., 2001; Mashkovtsev and Smirnov, 2004).

The present study focuses on a new hydrothermally grown synthetic emerald manufactured since 2003 in Prague, Czech Republic. This new gem material, called Malossi synthetic emerald (figure 1), has been marketed since December 2004 in Italy by Arsaurea Gems (Milan) and in the U.S. by Malossi Inc., the U.S. subsidiary of Malossi Created Gems (Raleigh, North Carolina). Currently, about 5,000–6,000 carats of the faceted synthetic emeralds are produced per year, and this rate is expected to increase (A. Malossi, pers. comm., 2005). The crystals produced so far range from 25 to 150 ct, with a mean weight of about 77 ct, and the largest faceted stone obtained weighs about 15 ct (A. Malossi, pers. comm., 2005). In this article, we report those fea-

tures of Malossi synthetic emeralds that can be used to distinguish this material from natural and other synthetic (hydrothermal and flux) emeralds.

GROWTH TECHNIQUE

Malossi synthetic emeralds are grown at about 450°C in a small rotating autoclave that is lined with gold and carefully sealed. A seed of natural yellow beryl, suspended by a platinum wire, is used to help initiate growth. Concentrated hydrochloric acid is usually used to prevent Cr (the only chromophore used) from precipitating. Large crystals of the synthetic emerald can be grown in 40–60 days (A. Malossi, pers. comm., 2005).

MATERIALS AND METHODS

For this study, we examined 30 emerald-cut gems and 5 rough samples of the new synthetic emerald,

See end of article for About the Authors and Acknowledgments.
GEMS & GEMOLOGY, Vol. 41, No. 4, pp. 328–338.
© 2005 Gemological Institute of America



Figure 1. Malossi synthetic emeralds are grown by a hydrothermal technique in the Czech Republic, using Italian technology. These crystals (28.40–141.65 ct and 7.1–69.9 mm) and emerald cuts (1.34–7.89 ct) are some of the samples examined for this study. Photo by Alberto Malossi.

which were provided by A. Malossi (see, e.g., figure 1). The faceted samples weighed 1.34–7.89 ct, and the rough specimens ranged from 28.40 to 141.65 ct ($30.0\text{--}69.9 \times 10.8\text{--}22.5 \times 7.1\text{--}14.8$ mm). Representative faceted samples of hydrothermal synthetic emeralds from other commercial sources (all from the collection of the Italian Gemological Institute) were studied for comparison: Russian (5), Biron (5), and Linde-Regency (1). In addition, literature comparisons were made to other synthetic emeralds produced by the hydrothermal technique (Chinese, Lechleitner), as well as to flux synthetics and natural emeralds.

All the faceted samples were examined by standard gemological methods to determine their optical properties (refractive indices, birefringence, and pleochroism), specific gravity, UV fluorescence, and microscopic features.

Preliminary qualitative and semiquantitative chemical analyses of 11 faceted synthetic specimens (8 Malossi, 1 Russian, 1 Biron, and 1 Linde-Regency) were obtained by a Cambridge Stereoscan 360 scanning electron microscope, equipped with an Oxford Isis 300 energy-dispersive X-ray spectrometer, for the following elements: Si, Al, V, Cr, Fe, Ni, Cu, Na, Mg, and Cl. Quantitative chemical data (for the same elements) were obtained from these same 11 samples using an Applied Research Laboratories electron microprobe fitted with five wavelength-dispersive spectrometers and a Tracor Northern energy-dispersive spectrometer.

Room-temperature nonpolarized spectroscopy in the visible (460–750 nm), near-infrared (13000–4000 cm^{-1}), and mid-infrared (4000–400 cm^{-1}) regions was carried out on all Malossi, Russian, Biron, and Linde-Regency samples. We used a Nicolet NEXUS FTIR-Vis spectrometer, equipped with a diffuse reflectance accessory (DRIFT), which had a resolution of 4 and 8 cm^{-1} in the infrared and visible ranges, respectively.

Mid-infrared spectroscopy (4000–400 cm^{-1}) was also carried out in transmission mode using KBr compressed pellets with a 1:100 ratio of sample:KBr. Since this is a destructive technique, we restricted these IR measurements to portions of two rough specimens only.

Additional UV-Vis-NIR reflectance spectra were recorded by an Avantes BV (Eerbeek, the Netherlands) apparatus equipped with halogen and deuterium lamps and a CCD spectrometer with four gratings (200–400 nm, 400–700 nm, 700–900 nm, and 900–1100 nm), a 10 μm slit, and a spectral resolution of 0.5 nm. A polytetrafluoroethylene disk (reflectance about 98% in the 400–1500 nm range) was used as a reference sample.

X-ray powder diffraction was also used to investigate an incrustation on the surface of one Malossi synthetic emerald crystal. Measurements were performed at room temperature, by means of a Bragg-Brentano para-focusing X-ray powder diffractometer Philips X'Pert, in the θ – θ mode, with $\text{CuK}\alpha$ radiation ($\lambda = 1.5418$ Å), over the range of 5° to 75° 2θ .

RESULTS AND DISCUSSION

Gemological Testing. The standard gemological properties obtained on the 30 faceted Malossi samples are summarized in table 1. All the samples were transparent, with a bluish green color. They exhibited strong dichroism in yellowish green and bluish green.

Their R.I. and S.G. values: (1) overlapped those of their natural counterparts, especially low-alkali emeralds from various geographic localities (such as Colombia and Brazil; Schrader, 1983); (2) were similar to those we measured in Biron and Linde-Regency synthetics, and to those reported for Lechleitner and Chinese synthetic emeralds (Flanigen et al., 1967; Kane and Liddicoat, 1985; Schmetzer, 1990; Webster, 1994; Schmetzer et al., 1997; Sechos, 1997; Chen et al., 2001); but (3) were lower than those of our Russian synthetic samples (in agreement with Schmetzer, 1988; Webster, 1994; Koivula et al., 1996; Sechos, 1997). Most flux-grown synthetic emeralds from various manufacturers have R.I., birefringence, and S.G. values that are lower than those observed in the Malossi samples (for comparison, see Flanigen et al., 1967; Schrader, 1983; Kennedy, 1986; Graziani et al., 1987). The pleochroism and Chelsea filter reaction of the Malossi samples were not diagnostic of synthetic origin.

The various synthetics showed significant differences in their fluorescence to UV radiation: Malossi synthetic emeralds belonged to a group exhibiting red UV fluorescence that includes Linde-Regency and Chinese products, whereas Russian and Biron synthetic emeralds are inert to long- and short-wave

TABLE 1. Gemological properties of Malossi hydrothermal synthetic emeralds.

Color	Bluish green
Diaphaneity	Transparent
Optic character	Uniaxial negative
Refractive indices	$n_o = 1.573\text{--}1.578$ $n_e = 1.568\text{--}1.570$
Birefringence	0.005–0.008
Specific gravity	2.67–2.69
Pleochroism	Strong dichroism: o-ray = yellowish green e-ray = bluish green
Chelsea filter reaction	Strong red
UV fluorescence	Short-wave: moderate red Long-wave: weak red
Internal features	Crystals (probably synthetic phenakite), "fingerprints," two-phase inclusions, growth tubes, fractures, various forms of growth structures, color zoning, seed plates, irregular growth zoning



Figure 2. Straight, parallel growth bands, which also may be present in natural emeralds, are seen in this faceted Malossi synthetic emerald. Photomicrograph by Renata Marcon; magnified 30x.

UV radiation. The fluorescence of Malossi synthetic emeralds might hint at a synthetic origin, although a few high-Cr and low-Fe Colombian emeralds also have red UV fluorescence (Graziani et al., 1987).

The Malossi synthetic emeralds showed a variety of internal features when viewed with a gemological microscope. Growth patterns of various forms (straight, parallel, uniform, angular, and intersecting), often associated with color zoning, were widespread in some of the crystals and cut stones (e.g., figure 2). Irregular growth structures (figure 3), similar to those observed in other hydrothermal synthetic emeralds, were seen in almost all the samples, providing evidence of hydrothermal synthesis. Six of the faceted Malossi synthetic emeralds contained seed plates (fig-

Figure 3. Irregular growth structures are also seen in Malossi synthetic emeralds. Such features provide evidence of a hydrothermal synthetic origin. Note also the natural-appearing "fingerprints" in this sample. Photomicrograph by Renata Marcon; magnified 35x.

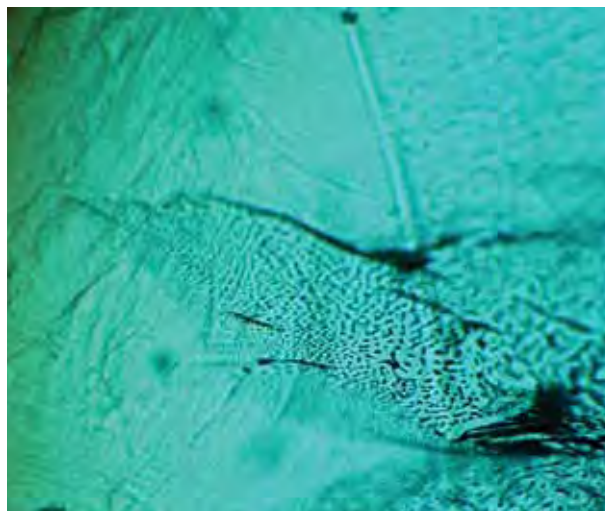




Figure 4. A seed plate (with obvious fluid inclusions) forms the table of this faceted Malossi synthetic emerald (3.92 ct). Photomicrograph by Renata Marcon.

ure 4; this seed plate had $n_e = 1.568$, $n_o = 1.573$, and a birefringence of 0.005). In some cases, irregular growth zoning was seen in the synthetic overgrowth adjacent to the seed plates. The presence of a seed plate is proof of synthetic origin.

“Fingerprints” and two-phase (liquid and gas) inclusions were observed in most of the Malossi samples (again, see figure 3 and figure 5). In some cases, these inclusions were similar to those observed in natural emeralds, in contrast to flux-grown synthetics, in which any fingerprint-like inclusions consist of fractures that are healed by flux filling. Fractures were also common in the Malossi synthetic emeralds, but they do not provide any evidence of synthetic origin. Two Malossi samples contained small cone-shaped growth tubes, filled with a fluid, similar to those that were recently documented in a natural emerald (Choudhary, 2005). Prismatic, transparent,

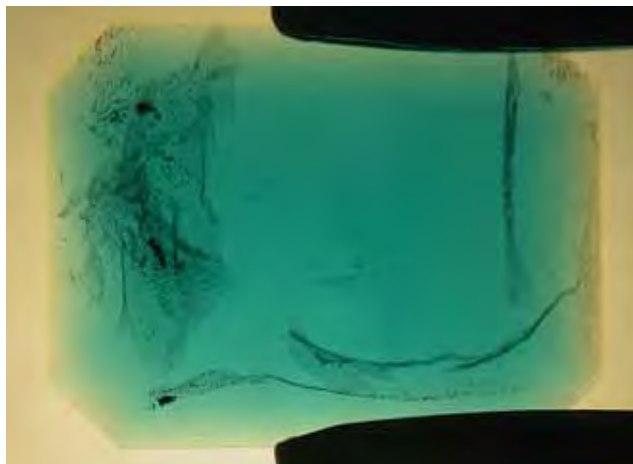
and colorless crystals—alone or in aggregates—were observed in four Malossi samples (figure 6). On the basis of their morphology, birefringence, and refractive index (higher than that of emerald), such crystalline inclusions are probably phenakite (Be_2SiO_4), which is somewhat common in hydrothermal synthetic emeralds (Flanigen et al., 1967) and also may provide evidence that the host emerald is synthetic (Kane and Liddicoat, 1985).

X-ray powder diffraction of an incrustation on the surface of one Malossi synthetic emerald crystal revealed the presence of phenakite and beryl, hinting at the occurrence of an incongruent precipitation of beryl (Nassau, 1980; Sinkankas, 1981). We did not observe the lamellar metallic inclusions that are sometimes present in other synthetic emeralds (e.g., gold, which is frequently found in Biron samples; Kane and Liddicoat, 1985).

Chemical Composition. Quantitative chemical analyses of eight Malossi synthetic emeralds (samples A to H) and three other hydrothermal synthetic emeralds (one each from Russian, Biron, and Linde-Regency production) are summarized in table 2.

Chromium was the only chromophore found in the Malossi samples. The following elements were below the detection limits of the electron microprobe: Na, Mg, V, Fe (in all but one sample), Ni, and Cu. Cl, probably from the growth solution (Nassau, 1980; Stockton, 1984; Kane and Liddicoat, 1985; see also Growth Technique section), was inhomogeneously distributed within the samples and between

Figure 5. This faceted Malossi synthetic emerald contains conspicuous “fingerprints” (left) that are composed of tiny two-phase (liquid/gas) inclusions (right). Photomicrographs by Renata Marcon; magnified 8× (left) and 60× (right, in darkfield illumination).



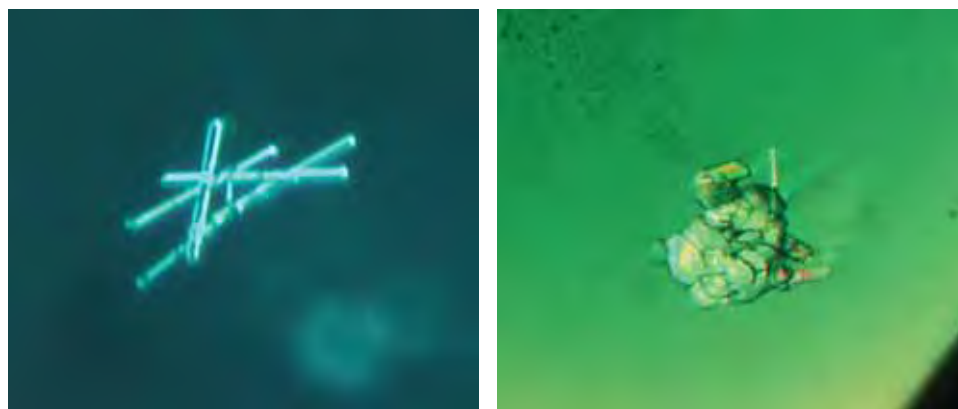


Figure 6. These images show examples of inclusion aggregates formed by transparent colorless prismatic crystals in Malossi synthetic emeralds. Their optical characteristics and occurrence in hydrothermal synthetic emerald suggest they are phenakite. Photomicrographs by Renata Marcon, in darkfield illumination (left, magnified 100×) and with crossed polarizers (right, magnified 50×).

different specimens, as shown in figure 7. The Cl content ranged up to 0.93 wt.%, with a mean value of 0.10 wt.%.

Figure 8 and table 2 compare the chemical properties of Malossi synthetic emeralds to those of representative samples from other hydrothermal producers. The chemical composition of Malossi synthetic

emeralds is distinctively different from Russian and Biron synthetics. In agreement with the results of Schmetzer (1988), Mashkovtsev and Solntsev (2002), and Mashkovtsev and Smirnov (2004), our Russian synthetic sample contained Cr, Fe, Ni, and Cu, but neither Cl nor V was detected. Although not tested for this study, Lechleitner synthetic emeralds report-

TABLE 2. Averaged electron-microprobe analyses of Malossi and other hydrothermal synthetic emeralds.^a

Chemical composition	Malossi samples								Russian	Biron	Linde-Regency
	A	B	C	D	E	F	G	H			
No. analyses	8	6	13	4	9	5	6	5	9	5	7
Oxides (wt.%)											
SiO ₂	66.21	66.00	66.01	65.81	65.34	65.72	64.50	66.02	64.33	64.09	65.83
Al ₂ O ₃	18.96	19.01	19.69	19.42	18.81	18.14	18.28	19.35	16.77	18.56	19.05
V ₂ O ₃	bdl	bdl	bdl	bdl	bdl	bdl	bdl	bdl	bdl	0.75	bdl
Cr ₂ O ₃	0.36	0.43	0.51	0.60	0.82	1.96	1.01	0.66	0.34	0.75	0.78
Fe ₂ O ₃ ^b	bdl	0.06	bdl	bdl	bdl	bdl	bdl	bdl	3.31	bdl	bdl
NiO	bdl	bdl	bdl	bdl	bdl	bdl	bdl	bdl	0.24	bdl	bdl
CuO	bdl	bdl	bdl	bdl	bdl	bdl	bdl	bdl	0.18	bdl	bdl
Cl	0.21 ^c	0.09 ^c	0.14 ^c	0.03 ^c	0.05	0.06	0.06	0.09	bdl	0.31	0.18
BeO ^d	13.79	13.74	13.74	13.70	13.60	13.68	13.43	13.74	13.39	13.35	13.70
Total	99.53	99.33	100.09	99.56	98.62	99.56	97.28	99.86	98.56	97.81	99.54
Cl range	0.07–0.93	0.04–0.14	0.03–0.87	bdl–0.06	0.03–0.11	0.02–0.11	bdl–0.14	bdl–0.25	bdl–0.05	0.28–0.36	0.12–0.34
Cr ₂ O ₃ range	0.18–1.17	0.36–0.51	0.42–0.59	0.58–0.63	0.76–0.87	1.37–3.53	0.96–1.07	0.63–0.71	0.25–0.40	0.74–0.79	0.49–0.94
Ions per 6 Si atoms											
Si	6.000	6.000	6.000	6.000	6.000	6.000	6.000	6.000	6.000	6.000	6.000
Al	2.025	2.037	2.109	2.087	2.036	1.952	2.004	2.072	1.843	2.048	2.046
V	bdl	bdl	bdl	bdl	bdl	bdl	bdl	bdl	bdl	0.083	bdl
Cr	0.026	0.031	0.037	0.043	0.060	0.141	0.074	0.047	0.025	0.056	0.056
Fe	bdl	0.004	bdl	bdl	bdl	bdl	bdl	bdl	0.232	bdl	bdl
Ni	bdl	bdl	bdl	bdl	bdl	bdl	bdl	bdl	0.018	bdl	bdl
Cu	bdl	bdl	bdl	bdl	bdl	bdl	bdl	bdl	0.013	bdl	bdl
Cl	0.032	0.014	0.022	0.005	0.008	0.009	0.009	0.014	bdl	0.049	0.028

^a Instrument operating conditions: accelerating voltage = 15 kV, sample current = 15 nA, count time = 20 seconds on peaks and 5 seconds on background, beam spot size = 15 μm. Standards: natural omphacite (for Si, Fe, Al, Na, Mg) and sodalite (for Cl); pure V, Cr, Ni, and Cu were used for those elements. Abbreviation: bdl = below detection limit (in wt.%): 0.05 V₂O₃, 0.04 Fe₂O₃, 0.11 NiO, 0.10 CuO, 0.02 Cl. Sodium and magnesium were below the detection limits in all analyses (0.01 wt.% Na₂O and 0.03 wt.% MgO).

^b Total iron is calculated as Fe₂O₃.

^c Average Cl content was calculated for 6, 4, 12, and 3 points, respectively, for samples A, B, C, and D.

^d Calculated assuming Be/Si=0.5.

edly have a similar composition (Hänni, 1982; Schmetzer, 1990). In our Biron sample, V and Cr (acting as chromophores) were found along with Cl, which is consistent with previously published results (Stockton, 1984; Kane and Liddicoat, 1985; Mashkovtsev and Solntsev, 2002; and Mashkovtsev and Smirnov, 2004). The Linde-Regency synthetic emerald was characterized by the presence of Cr and Cl (see also Hänni, 1982; Stockton, 1984), similar to the Malossi material. However, the Cl content in the Malossi samples was generally less than 0.12 wt.%, as shown in figure 7, whereas the Cl in our Linde-Regency sample was never below 0.12 wt.%, in keeping with the results of Hänni (1982), who found a Cl content of 0.3–0.4 wt.% in Linde synthetic emeralds. Cr and Cl also were recorded in the two different generations of Chinese hydrothermal synthetic emeralds examined by Schmetzer et al. (1997) and Chen et al. (2001). Schmetzer et al. (1997) indicated an average Cl content of ≈ 0.68 wt.%, in an earlier Chinese synthetic production, whereas Chen et al. (2001) reported Cl ≈ 0.15 wt.%, in the later generation, in addition to a significant Na_2O content (>1 wt.%). The earlier Chinese production contains more Cl than the

Figure 7. The Cl contents measured in eight Malossi synthetic emeralds (each represented by a different color) are shown here. Most of the analyses contain less than 0.12 wt.% Cl (detection limit of Cl is 0.02 wt.%). For average Cl data, see table 2. Enriched contents of Cl were recorded in a few of the analyses, which illustrates the compositional inhomogeneity of the samples.

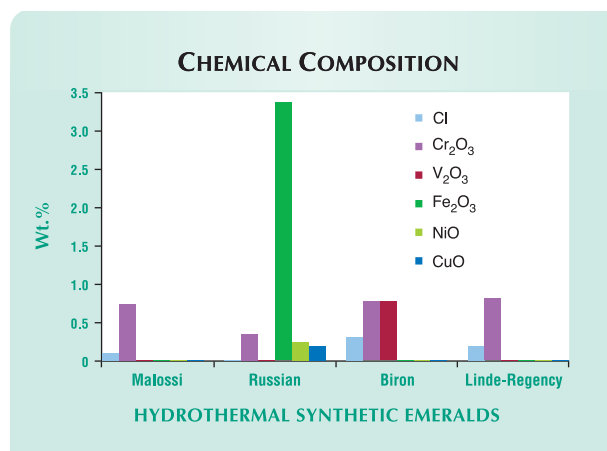
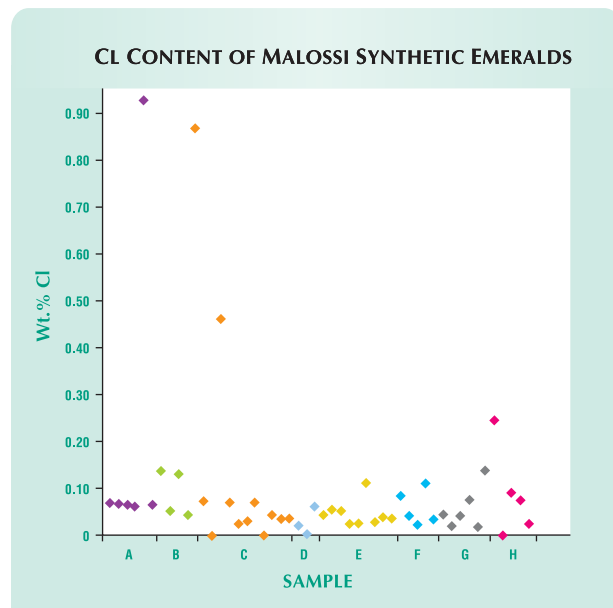


Figure 8. The average contents of Cl, Cr, V, Fe, Ni, and Cu are shown here for Malossi synthetic emeralds compared to representative samples of Russian, Biron, and Linde-Regency hydrothermal synthetics examined as part of this study. The Malossi and Linde-Regency samples have similar chemical features, which are distinctively different from the Russian and Biron synthetics.

Malossi material; the later Chinese synthetic emerald is distinguishable from Malossi synthetics by the presence of Na.

As previously reported by Hänni (1982), Schrader (1983), and Stockton (1984), chemical composition can be of great importance in separating synthetic and natural emeralds. In the case of Malossi synthetic emerald, the presence of chlorine—which typically is not found in significant amounts in natural emerald—can be an important indicator. Yu et al. (2000) reported Cl in some natural emeralds, typically at low concentrations, although some Colombian and Zambian samples contained up to 0.19 wt.% Cl. Thus, a Cl content above 0.2 wt.% provides a strong indication of hydrothermal synthetic origin. The Fe-free Malossi synthetic emeralds (except sample B, with a trace of Fe) were similar in composition to some Fe-poor natural emeralds from certain localities (such as Colombia), but they are easily distinguishable from Fe-rich natural emeralds (such as Brazilian, Zambian, and Austrian stones; see Hänni, 1982; Schrader, 1983; Stockton, 1984; Yu et al., 2000). The absence of any significant Na and Mg in Malossi synthetic emeralds (≤ 0.01 and ≤ 0.03 wt.% oxide, respectively) can be used to separate these stones from alkali-rich natural emeralds (Hänni, 1982; Schrader, 1983).

Electron-microprobe analyses of a seed plate in a Malossi sample (again, see figure 4) revealed an appreciable iron content (0.40 wt.% Fe_2O_3), whereas Cr, V, and Cl were below the detection limits. This

composition, combined with the R.I. values of the seed plate, is consistent with the producer's claim that natural yellow beryl is used for the seed material (compare to Sinkankas, 1981; Aliprandi and Guidi, 1987; Webster, 1994).

Spectroscopy. The results of UV-Vis-NIR and IR spectroscopy are summarized in table 3, including a comparison to natural and other synthetic emeralds.

Mid-infrared spectra (4000–2000 cm^{-1}) in diffuse reflectance mode are shown in figure 9. A series of intense peaks between 4000 and 3400 cm^{-1} in all the

synthetic emeralds we studied is related to their high water contents (Stockton, 1987; Schmetzer et al., 1997). Such features are characteristic of both natural and hydrothermal synthetic emeralds, but they are not found in flux synthetic samples (Stockton, 1987).

Bands in the range 3100–2500 cm^{-1} , commonly used to identify hydrothermal synthetic emeralds (Schmetzer et al., 1997; Mashkovtsev and Smirnov, 2004), were observed in our Malossi samples, as well as in those from Biron and Linde-Regency (see also Stockton, 1987; Mashkovtsev and Solntsev, 2002; Mashkovtsev and Smirnov, 2004). Schmetzer

TABLE 3. Main spectroscopic features of Malossi and other synthetic as well as natural emeralds.

Spectral region	Hydrothermal synthetic emeralds ^a				Flux synthetic emeralds ^b	Natural emeralds ^{b,c}
	Malossi	Russian	Biron	Linde-Regency		
Mid-IR (4000–2000 cm^{-1})	Intense absorption between 4000 and 3400 cm^{-1} , associated with high water content Band at 3295 cm^{-1} , with shoulder at 3232 cm^{-1} , probably related to vibration of N-H bonds Group of bands in the 3100–2500 cm^{-1} range, associated with Cl	Intense absorption between 4000 and 3400 cm^{-1} , associated with high water content	Intense absorption between 4000 and 3400 cm^{-1} , associated with high water content Group of bands in the 3100–2500 cm^{-1} range, associated with Cl	Intense absorption between 4000 and 3400 cm^{-1} , associated with high water content Band at 3295 cm^{-1} , with shoulder at 3232 cm^{-1} , probably related to vibration of N-H bonds Group of bands in the 3100–2500 cm^{-1} range, associated with Cl	(none reported)	Intense absorption between 4000 and 3400 cm^{-1} , associated with high water content
Near-IR (9000–4000 cm^{-1})	Combination bands and overtones of water molecules	Combination bands and overtones of water molecules Broad band at 8475 cm^{-1} , related to Cu^{2+}	Combination bands and overtones of water molecules	Combination bands and overtones of water molecules	(none reported)	Combination bands and overtones of water molecules
UV-Vis-NIR (300–1000 nm)	Cr^{3+} absorption features at 430, 476, 600, 637, 646, 662, 681, and 684 nm	Cr^{3+} absorption features at 430, 476, 600, 637, 646, 662, 681, and 684 nm Band at 373 nm, associated with Fe^{3+} Band at 760 nm, related to Cu^{2+}	Cr^{3+} absorption features at 430, 476, 600, 637, 646, 662, 681, and 684 nm	Cr^{3+} absorption features at 430, 476, 600, 637, 646, 662, 681, and 684 nm	Cr^{3+} absorption features at 430, 476–477, 600, 637, 646, 660–662, 680, and 683 nm	Cr^{3+} absorption features at (420), 430–431, 476, 600–602, (629), 637, 645, 662, 680, and 683–685 nm (Bands at 370 and 423 nm, associated with Fe^{3+}) (Bands at 820 and 833 nm, related to Fe^{2+}) ($\text{Fe}^{2+}/\text{Fe}^{3+}$ intervalence charge transfer absorption band between 599 and 752 nm)

^a Based on results from the present study.

^b Data from the gemological literature (Wickersheim and Buchanan, 1959; Wood and Nassau, 1967, 1968; Farmer, 1974; Kennedy, 1986; Graziani et al., 1987; Stockton, 1987; Schmetzer, 1988).

^c Features in parentheses are not seen in all natural emeralds.

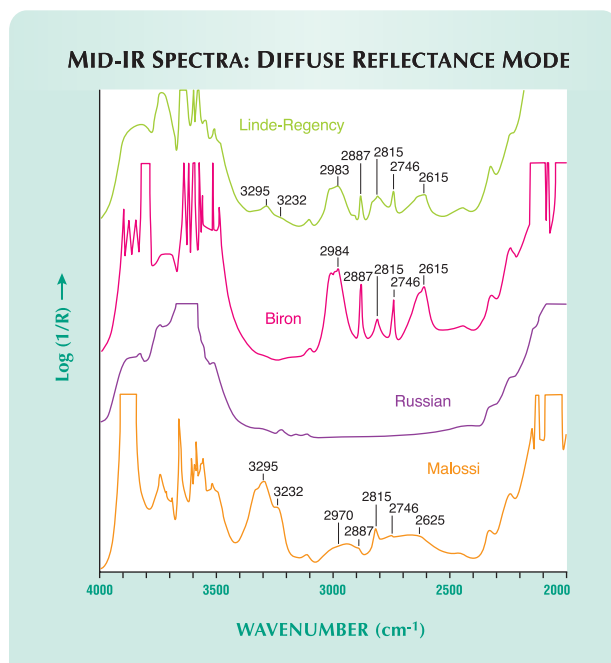


Figure 9. Mid-infrared spectra (4000–2000 cm^{-1}) in diffuse reflectance mode are shown for the Malossi, Russian, Biron, and Linde-Regency hydrothermal synthetic emeralds tested for this study. The spectra exhibit several differences, particularly in the band at 3295 cm^{-1} with the associated shoulder at 3232 cm^{-1} that is so pronounced in the Malossi material. (The maxima above 3500 cm^{-1} and below 2200 cm^{-1} appear flat because of total absorption in these areas).

et al. (1997) found these bands in Chinese samples as well. However, Russian and Lechleitner synthetic emeralds are transparent over the same energy range (Stockton, 1987; Koivula et al., 1996; Mashkovtsev and Solntsev, 2002; Mashkovtsev and Smirnov, 2004; see also figure 9). Schmetzer et al. (1997) attributed these bands to Cl, in agreement with more recent results by Mashkovtsev and Solntsev (2002) and Mashkovtsev and Smirnov (2004), who specifically cited HCl molecules in the hexagonal channels of the beryl structure. This interpretation is consistent with the chemical compositions we determined for Malossi, Biron, and Linde-Regency synthetics and with the producer's statement that Malossi synthetic emeralds are grown in a solution of HCl.

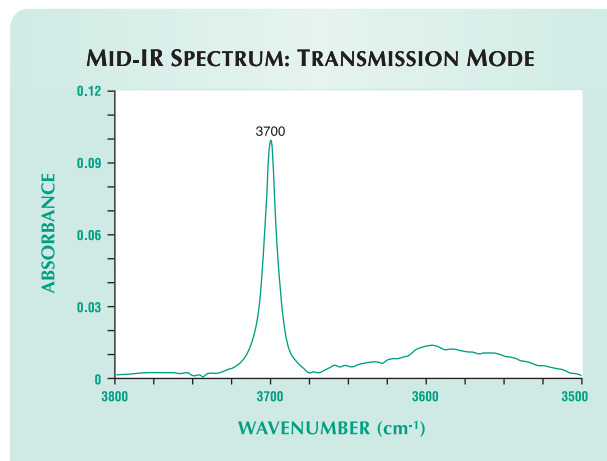
An additional band at 3295 cm^{-1} , with a shoulder at 3232 cm^{-1} , occurred in both the Malossi and Linde-Regency products (Stockton, 1987; Mashkovtsev and Solntsev, 2002; Mashkovtsev and Smirnov, 2004; see also figure 9). Mashkovtsev and Solntsev (2002) and Mashkovtsev and Smirnov (2004) attributed this feature to the vibrational

stretching mode of the N-H bond (for details, see also references cited in these two articles), which is consistent with the known use of ammonium halides in the solutions employed for emerald synthesis (Nassau, 1980).

The “type” of water molecules in Malossi synthetic emeralds can be determined by (destructive) mid-infrared spectroscopy in transmission mode (see box A in Schmetzer et al., 1997, for the advantages of transmission IR spectroscopy). In the diagnostic range of 3800–3500 cm^{-1} , we recorded a single sharp absorption band at 3700 cm^{-1} (figure 10), which indicates that H_2O molecules in Malossi stones are type I (i.e., their H–H vector is parallel to the c-axis in alkali-free beryl samples; Wood and Nassau, 1967, 1968; Charoy et al., 1996; Kolesov and Geiger, 2000; Gatta et al., in press). All this is in keeping with the absence of any significant alkali content in Malossi material, which agrees with results reported by Kolesov and Geiger (2000), who observed the same single mode at 3700 cm^{-1} in other hydrous synthetic beryl crystals. However, relatively recent spectroscopic and neutron diffraction studies (Artioli et al., 1995; Charoy et al., 1996; Kolesov and Geiger, 2000; Gatta et al., in press) suggest that there are some uncertainties about the vibrational behavior and orientation of H_2O molecules in various beryl samples.

Nonpolarized near-infrared spectra (9000–4000 cm^{-1}) in diffuse reflectance mode of our Malossi,

Figure 10. The mid-infrared spectrum (3800–3500 cm^{-1}) in transmission mode of a pressed pellet containing powdered Malossi synthetic emerald shows a peak at 3700 cm^{-1} that is related to the presence of type I water molecules.



NEAR-IR SPECTRA: DIFFUSE REFLECTANCE MODE

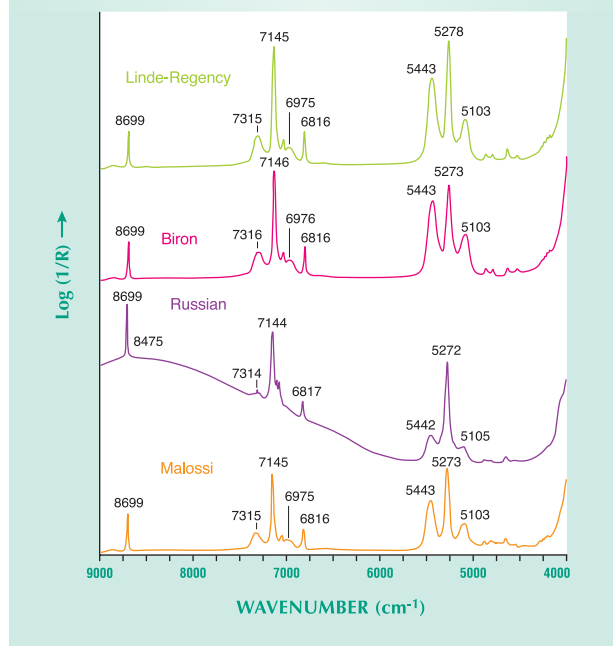


Figure 11. Near-infrared spectra (9000–4000 cm^{-1}) in diffuse reflectance mode are shown for the Malossi, Russian, Biron, and Linde-Regency hydrothermal synthetic emeralds studied. The spectra of all samples exhibit combination bands and overtones of water molecules, which are typical features of both hydrothermal synthetic and natural emeralds.

Russian, Biron, and Linde-Regency synthetic emeralds are displayed in figure 11. All samples show combination bands and overtones of water molecules (Wickersheim and Buchanan, 1959; Wood and Nassau, 1967, 1968; Farmer, 1974). These features are also typical of natural emeralds (see references above), whereas they are always lacking in flux synthetic emeralds. Russian hydrothermal synthetic emeralds exhibit a broad band at 8475 cm^{-1} (see also Koivula et al., 1996; Mashkovtsev and Smirnov, 2004) related to an optical transition involving Cu^{2+} ions (Mashkovtsev and Smirnov, 2004) that is commonly absent in hydrothermal specimens from other producers.

Nonpolarized UV-Vis-NIR absorption spectra of our Malossi, Russian, Biron, and Linde-Regency hydrothermal synthetic emeralds (figure 12) confirm the presence of Cr^{3+} through the occurrence of two broad bands at 430 and 600 nm; peaks at 476, 637, 646, and 662 nm; and a doublet at 681–684 nm (see Wood and Nassau, 1968; Rossman, 1988; Schmetzer, 1988, 1990), similar to natural and flux

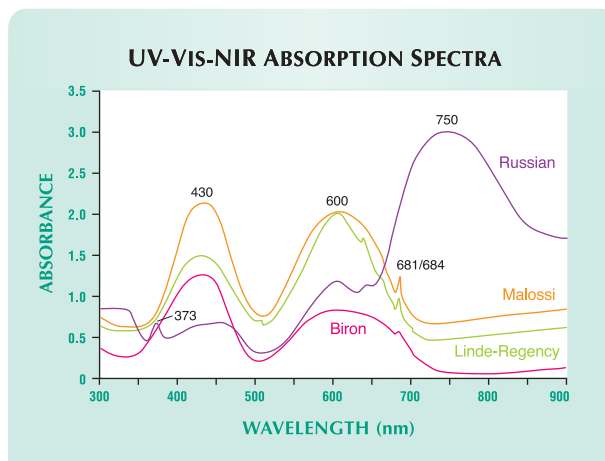
synthetic emeralds. Given that the absorption peaks of Cr^{3+} and V^{3+} are very close to one another (see references above and Burns, 1993), it is not possible to reliably discriminate the patterns of Malossi and Linde-Regency synthetic stones (Cr-bearing only) from those of Biron synthetic samples (Cr- and V-bearing). However, Russian synthetic emeralds show differences from the other hydrothermal synthetics: a broad band at about 750 nm, which Schmetzer (1988, 1990) related to Cu^{2+} , as well as an absorption at 373 nm, which he associated with Fe^{3+} . In natural iron-bearing emeralds, absorption bands for Fe^{3+} , Fe^{2+} , and $\text{Fe}^{2+}/\text{Fe}^{3+}$ may also be present (Schmetzer, 1988; again, see table 3).

IDENTIFICATION

Separation from Natural Emeralds. Malossi synthetic emeralds have a number of characteristics that, in combination, allow them to be separated from natural emeralds:

1. **Microscopic features:** Irregular growth structures (observed in almost all Malossi synthetic emeralds), natural seed plates (used to initiate growth), and phenakite-like crystals (hinting at the occurrence of an incongruent beryl precipitation) provide evidence of hydrothermal synthesis.

Figure 12. The nonpolarized UV-Vis-NIR (300–900 nm) absorption spectra of the Malossi, Russian, Biron, and Linde-Regency hydrothermal synthetic emeralds tested all show Cr^{3+} absorption bands. Only the Russian sample exhibits other significant features, such as a peak at 373 nm (related to Fe^{3+}) and a broad band at about 750 nm (associated with Cu^{2+}).



2. *Chemical composition:* The presence of Cl, combined with the absence of any significant amounts of Fe, Na, and Mg, provides a useful tool for the separation from Fe-alkali-bearing natural emeralds. In the case of Fe-Na-Mg-poor natural samples (such as Colombian stones), a Cl content >0.2 wt.% can be used to identify the Malossi synthetics, although due to possible compositional overlap, chemical analysis alone is not a reliable proof of synthesis.

3. *Spectroscopic measurements:* Mid-infrared bands in the 3100–2500 cm^{-1} range (related to Cl) and a band at 3295 cm^{-1} with an associated shoulder at 3232 cm^{-1} , are further diagnostic features of synthetic origin.

In summary, Malossi synthetic emeralds are readily separated from most natural Fe- and/or alkali-bearing emeralds, whereas a combination of the diagnostic features discussed above is required to distinguish them from Fe- and alkali-poor natural emeralds.

Separation from Other Synthetic Emeralds. Malossi, like all other hydrothermal synthetic emeralds, are readily separated from flux synthetic emeralds because the latter (1) have lower refractive index (from 1.556), birefringence (from 0.003), and specific gravity (from 2.64) values; (2) contain typical flux inclusions; and (3) do not exhibit water-related bands in the mid- (between 4000 and 3400 cm^{-1}) and near- (9000–5000 cm^{-1}) IR spectra.

Malossi synthetic emeralds, which are Cr- and Cl-bearing, differ from the Russian, Lechleitner, and Biron hydrothermal synthetic emeralds studied to date on the basis of chemical composition. Russian and Lechleitner synthetics have Cr, Fe, Cu, and Ni, while Biron has V in addition to Cr and Cl. These differences can be seen in their gemological and spectroscopic properties. The separation of Malossi from Chinese synthetic emeralds may be possible based on either a larger amount of Cl in the earlier-generation Chinese material or the presence of Na in the later-generation Chinese synthetics. Also, according to information given by Chinese gemologists at the Fall 2004 International Gemological Congress in Wuhan (China), the production of Chinese hydrothermal synthetic emeralds has been discontinued (K. Schmetzer, pers. comm., 2005). The chemical separation of Malossi from Linde-



Figure 13. Faceted Malossi synthetic emeralds have been commercially available in Italy and in the U.S. since December 2004. These emerald cuts (4.00 ct, left, and 2.20 ct, right) are set in rings together with synthetic moissanite. Composite photo by Alberto Malossi.

Regency hydrothermal synthetic emeralds is less straightforward and further research is needed.

CONCLUSIONS

A new type of hydrothermal synthetic emerald is now being produced in the Czech Republic with Italian technology. These Malossi synthetic emeralds have been commercially available since December 2004 (figure 13). This material belongs to the group of Cl-bearing, alkali-free hydrothermal synthetic emeralds, with Cr^{3+} as the only chromophore. Water is present as type I molecules.

Malossi synthetic emerald can be distinguished from its natural counterpart on the basis of microscopic features (in particular, irregular growth structures, seed plates, and/or phenakite-like crystals), as well as by the presence of Cl combined with the absence of significant Fe, Na, or Mg. In addition, mid-infrared spectroscopy reveals diagnostic bands in the 3100–2500 cm^{-1} range and at 3295 cm^{-1} (with a shoulder at 3232 cm^{-1}).

Malossi hydrothermal synthetic emerald can be easily discriminated from its flux synthetic counterparts, primarily on the basis of the absence of water molecules in the latter. The separation from Russian, Lechleitner, Chinese, and Biron hydrothermal synthetic emeralds can be made on the basis of chemical composition. The discrimination from Linde-Regency hydrothermal synthetic emeralds is more ambiguous, and further research is needed.

ABOUT THE AUTHORS

Miss Adamo (ilaria.adamo@unimi.it) and Mr. Merlini are Ph.D. students, and Dr. Pavese is professor of mineralogy, in the Earth Sciences Department at the University of Milan, Italy. Dr. Pavese is also a member of the Environmental Processes Dynamics Institute (IDPA), Section of Milan, National Research Council (CNR), Italy. Dr. Prosperi is director of the Italian Gemological Institute laboratory, Sesto San Giovanni, Italy. Dr. Diella is senior research scientist at IDPA, Section of Milan. Dr. Gemmi is responsible for the electron microscopy laboratory in the Earth Sciences Department of the University of Milan. Dr. Ajó is research director at the Inorganic and Surface Chemistry Institute, CNR, Padua,

Italy, and is responsible for the CNR Coordination Group for Gemological Materials Research.

ACKNOWLEDGMENTS

The authors are grateful to Alberto Malossi (Arsaurea Gems, Milan) for providing samples and information about these new hydrothermal synthetic emeralds. Agostino Rizzi (IDPA, CNR, Milan) and Dr. Renata Marcon (Italian Gemological Institute, Rome) are acknowledged for SEM-EDS analyses and photomicrographs, respectively. The authors are indebted to Dr. Karl Schmetzer (Petershausen, Germany) for a critical review of the manuscript before submission.

REFERENCES

- Aliprandi R., Guidi G. (1987) The two-colour beryl from Orissa, India. *Journal of Gemmology*, Vol. 20, No. 6, pp. 352–355.
- Artioli G., Rinaldi R., Wilson C.C., Zanazzi P.F. (1995) Single-crystal pulsed neutron diffraction of a highly hydrous beryl. *Acta Crystallographica*, Vol. B51, pp. 733–737.
- Burns R.G. (1993) *Mineralogical Applications of Crystal Field Theory*, 2nd ed. Cambridge Topics in Mineral Physics and Chemistry, Cambridge University Press, Cambridge, UK.
- Charoy B., De Donato P., Barres O., Pinto-Coelho C. (1996) Channel occupancy in an alkali-poor beryl from Serra Branca (Goiás, Brazil): Spectroscopic characterization. *American Mineralogist*, Vol. 81, No. 3/4, pp. 395–403.
- Chen Z.Q., Zeng J.L., Cai K.Q., Zhang C.L., Zhou W. (2001) Characterization of a new Chinese hydrothermally grown emerald. *Australian Gemmologist*, Vol. 21, No. 2, pp. 62–66.
- Choudhary G. (2005) Gem News International: An unusual emerald with conical growth features. *Gems & Gemology*, Vol. 41, No. 3, pp. 265–266.
- Farmer V.C. (1974) *The Infrared Spectra of Minerals*. Mineralogical Society, London.
- Flanigen E.M., Breck D.W., Mumbach N.R., Taylor A.M. (1967) Characteristics of synthetic emeralds. *American Mineralogist*, Vol. 52, No. 5/6, pp. 744–772.
- Gatta G.D., Nestola F., Bromiley G.D., Mattauca S. The real topological configuration of the extra-framework content in alkali-poor beryl: A multi-methodological study. *American Mineralogist*, in press.
- Graziani G., Gübelin E., Martini M. (1987) The Lennix synthetic emerald. *Gems & Gemology*, Vol. 23, No. 3, pp. 140–147.
- Hänni H.A. (1982) A contribution to the separability of natural and synthetic emeralds. *Journal of Gemmology*, Vol. 18, No. 2, pp. 138–144.
- Kane R.E., Liddicoat R.T. (1985) The Biron hydrothermal synthetic emerald. *Gems & Gemology*, Vol. 21, No. 3, pp. 156–170.
- Kennedy S.J. (1986) Seiko synthetic emerald. *Journal of Gemmology*, Vol. 20, No. 1, pp. 14–17.
- Koivula J.L., Kammerling R.C., DeGhionno D., Reinitz I., Fritsch E., Johnson M.L. (1996) Gemological investigation of a new type of Russian hydrothermal synthetic emerald. *Gems & Gemology*, Vol. 32, No. 1, pp. 32–39.
- Koivula J.L., Tannous M., Schmetzer K. (2000) Synthetic gem materials and simulants in the 1990s. *Gems & Gemology*, Vol. 36, No. 4, pp. 360–379.
- Kolesov B.A., Geiger C.A. (2000) The orientation and vibrational states of H₂O in synthetic alkali-free beryl. *Physics and Chemistry of Minerals*, Vol. 27, No. 8, pp. 557–564.
- Mashkovtsev R.I., Smirnov S.Z. (2004) The nature of channel constituents in hydrothermal synthetic emerald. *Journal of Gemmology*, Vol. 29, No. 3, pp. 129–141.
- Mashkovtsev R.I., Solntsev V.P. (2002) Channel constituents in synthetic beryl: Ammonium. *Physics and Chemistry of Minerals*, Vol. 29, No. 1, pp. 65–71.
- Nassau K. (1980) *Gems Made by Man*. Chilton Book Co., Radnor, PA.
- Rossmann G.R. (1988) Optical spectroscopy. In F.C. Hawthorne, Ed., *Spectroscopic Methods in Mineralogy and Geology*, Reviews in Mineralogy, Vol. 18, Mineralogical Society of America, Washington DC, pp. 207–254.
- Schmetzer K. (1988) Characterization of Russian hydrothermally grown synthetic emeralds. *Journal of Gemmology*, Vol. 21, No. 3, pp. 145–164.
- Schmetzer K. (1990) Two remarkable Lechleitner synthetic emeralds. *Journal of Gemmology*, Vol. 22, No. 1, pp. 20–32.
- Schmetzer K., Kiefert L., Bernhardt H.-J., Beili Z. (1997) Characterization of Chinese hydrothermal synthetic emerald. *Gems & Gemology*, Vol. 33, No. 4, pp. 276–291.
- Schrader H.-W. (1983) Contribution to the study of the distinction of natural and synthetic emerald. *Journal of Gemmology*, Vol. 18, No. 6, pp. 530–543.
- Sechos B. (1997) Identifying characteristics of hydrothermal synthetics. *Australian Gemmologist*, Vol. 19, No. 9, pp. 383–388.
- Sinkankas J. (1981) *Emerald and Other Beryls*. Chilton Book Co., Radnor, PA.
- Stockton C.M. (1984) The chemical distinction of natural from synthetic emerald. *Gems & Gemology*, Vol. 20, No. 3, pp. 141–145.
- Stockton C.M. (1987) The separation of natural from synthetic emerald by infrared spectroscopy. *Gems & Gemology*, Vol. 23, No. 2, pp. 96–99.
- Webster R. (1994) *Gems: Their Sources, Descriptions and Identification*, 5th ed. revised by P.G. Read. Butterworth-Heinemann, Oxford, England.
- Wickersheim K.A., Buchanan R.A. (1959) The near infrared spectrum of beryl. *American Mineralogist*, Vol. 44, No. 3/4, pp. 440–445.
- Wood D.L., Nassau K. (1967) Infrared spectra of foreign molecules in beryl. *Journal of Chemical Physics*, Vol. 47, No. 7, pp. 2220–2228.
- Wood D.L., Nassau K. (1968) The characterization of beryl and emerald by visible and infrared absorption spectroscopy. *American Mineralogist*, Vol. 53, No. 5/6, pp. 777–800.
- Yu K.N., Tang S.M., Tay T.S. (2000) PIXE studies of emeralds. *X-Ray Spectrometry*, Vol. 29, No. 4, pp. 267–278.

GEMS & GEMOLOGY

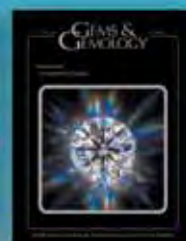
The Quarterly Journal
That Lasts A Lifetime



Spring 2004



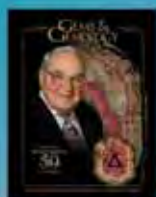
Summer 2004



Fall 2004



Winter 2004



Spring 2002/Special Issue



Summer 2002



Fall 2002



Winter 2002



Spring 2003



Summer 2003



Fall 2003



Winter 2003

Are you missing important information? **Order Your Back Issues Today!**

Limited Quantities Available

Spring 1997

Geophysics in Gemstone Exploration
Rubies and Fancy-Color Sapphires from Nepal
Properties of Near-Colorless Synthetic Diamonds

Summer 1997

Emeralds from Zimbabwe
Modern Diamond Cutting and Polishing
Rhodochrosite from Colorado

Fall 1997

Benitoite from San Benito County, California
Tairus Hydrothermal Synthetic Sapphires
Multicolored Bismuth-Bearing Tourmaline
from Lundazi, Zambia

Winter 1997

Understanding the Effect of Blue Fluorescence
on the Appearance of Diamonds
Synthetic Moissanite: A Diamond Substitute
Chinese Hydrothermal Synthetic Emerald

Spring 1998

Modern Diamond Cutting in India
Leigha—A Three-Dimensional Intarsia Sculpture
Russian Synthetic Pink Quartz

Summer 1998

Natural and Synthetic Rubies
Two Historical Objects from Basel Cathedral
Topaz, Aquamarine, and Other Beryls from
Namibia

Fall 1998

Modeling the Round Brilliant Cut Diamond:
An Analysis of Brilliance
Cultured Abalone Blister Pearls from
New Zealand
Estimating Weights of Mounted Colored Stones

Winter 1998

Natural-Color Type IIb Blue Diamonds
Fingerprinting of Two Diamonds Cut from the
Same Rough
Barite Inclusions in Fluorite

Spring 1999

The Identification of Zachery-Treated Turquoise
Russian Hydrothermal Synthetic Rubies and
Sapphires
The Separation of Natural from Synthetic
Colorless Sapphire

Summer 1999

On the Identification of Emerald Filling Substances
Sapphire and Garnet from Kalalani, Tanzania
Russian Synthetic Ametrine

Fall 1999—Special Issue

Special Symposium Proceedings Issue, including:
Observations on GE-Processed Diamonds,
Abstracts of Featured Speakers, Panel
Sessions, War Rooms, and Poster Sessions

Winter 1999

Classifying Emerald Clarity Enhancement at
the GIA Gem Trade Laboratory
Clues to the Process Used by General Electric
to Enhance the GE POL Diamonds
Diopside Needles as Inclusions in Demantoid
Garnet from Russia
Garnets from Madagascar with a Color
Change of Blue-Green to Purple

Spring 2000

Burmese Jade
Lapis Lazuli from Chile
Spectroscopic Evidence of GE POL Diamonds
Chromium-Bearing Taaffeites

Summer 2000

Characteristics of Nuclei in Chinese Freshwater
Cultured Pearls
Afghan Ruby and Sapphire
Yellow to Green HPHT-Treated Diamonds
New Lasering Technique for Diamond
New Oved Filling Material for Diamonds

Fall 2000

GE POL Diamonds: Before and After
Sapphires from Northern Madagascar
Pre-Columbian Gems from Antigua
Gem-Quality Haiyue from Germany

Winter 2000—Special Issue

Gem Localities of the 1990s
Enhancement and Detection in the 1990s
Synthetics in the 1990s
Technological Developments in the 1990s
Jewelry of the 1990s

Spring 2001

Ammolite from Southern Alberta, Canada
Discovery and Mining of the Argyle Diamond
Deposit, Australia
Hydrothermal Synthetic Red Beryl

Summer 2001

The Current Status of Chinese Freshwater
Cultured Pearls
Characteristics of Natural-Color and Heat-
Treated "Golden" South Sea Cultured Pearls
A New Method for Imitating Asterism

Fall 2001

Modeling the Appearance of the
Round Brilliant Cut Diamond: Fire
Pyrope from the Dora Maira Massif, Italy
Jeremejevit: A Gemological Update

Winter 2001

An Update on "Paraiba" Tourmaline
from Brazil
Spessartine Garnet from San Diego County,
California
Pink to Pinkish Orange Malaya Garnets from
Bekily, Madagascar
"Voices of the Earth": Transcending the
Traditional in Lapidary Arts

Spring 2002—Special Issue

The Ultimate Gemologist: Richard T. Liddicoat
Portable Instruments and Tips on Practical
Gemology in the Field
Liddicoatite Tourmaline from Madagascar
Star of the South: A Historic 128 ct Diamond

Summer 2002

Characterization and Grading of Natural-Color
Pink Diamonds
New Chromium- and Vanadium-Bearing
Garnets from Tranoroa, Madagascar
Update on the Identification of Treated
"Golden" South Sea Cultured Pearls

Fall 2002

Diamonds in Canada
"Diffusion Ruby" Proves to Be Synthetic Ruby
Overgrowth on Natural Corundum

Winter 2002

Chart of Commercially Available Gem Treatments
Gemesis Laboratory-Created Diamonds
Legal Protection for Proprietary Diamond Cuts
Rhodizite-Londonite from the Antsongombato
Pegmatite, Central Madagascar

Spring 2003

Photomicrography for Gemologists
Poudretteite: A Rare Gem from Mogok
Grandierite from Sri Lanka

Summer 2003

Beryllium Diffusion of Ruby and Sapphire
Seven Rare Gem Diamonds

Fall 2003

G. Robert Crowningshield:
A Legendary Gemologist
Cause of Color in Black Diamonds from Siberia
Obtaining U.S. Copyright Registration for the
Elara Diamond

Winter 2003

CVD Gem-Quality Synthetic Diamonds
Pezzottaite from Madagascar: A New Gem
Red Beryl from Utah: Review and Update

Spring 2004

Identification of CVD-Grown Synthetic Diamonds
Cultured Pearls from Gulf of California, Mexico
X-Ray Fingerprinting Routine for Cut Diamonds

Summer 2004

Gem Treatment Disclosure and U.S. Law
Lab-Grown Colored Diamonds from Chatham
The 3543 cm⁻¹ Band in Amethyst Identification

Fall 2004

Grading Cut Quality of Round Brilliant Diamonds
Amethyst from Four Peaks, Arizona

Winter 2004

Creation of a Suite of Peridot Jewelry: From the
Himalayas to Fifth Avenue
An Updated Chart on the Characteristics of
HPHT-Grown Synthetic Diamonds
A New Method for Detecting Be Diffusion-
Treated Sapphires (LIBS)

	U.S. Canada/Mexico International		
Single Issues*	\$12 ea.	\$15 ea.	\$18 ea.
Complete Volumes**			
1999, 2000 or 2002	\$45 ea.	\$55 ea.	\$65 ea.
1991-1998, 2001, 2003 and 2004	\$40 ea.	\$48 ea.	\$60 ea.
Three-year set	\$115 ea.	\$135 ea.	\$170 ea.
Five-year set	\$190 ea.	\$220 ea.	\$280 ea.

*Special Fall 1999, Winter 2000, and Spring 2002 issues are
\$18 (U.S.), \$21 (Canada & Mexico), \$24 (International).

**10% discount for GIA Alumni Association members.

E-Mail: gandg@gia.edu or visit www.gia.edu

To Order: Call Toll Free 800-421-7250 ext. 7142 or 760-603-4000 ext. 7142

Fax: 760-603-4595 or Write: G&G Subscriptions, P.O. Box 9022, Carlsbad, CA 92018-9022 USA

Some issues from 1981-1996 are also available. Please call for details on these and the 2005 issues as they are published.